Supporting Information

Yurtsever and Zewail 10.1073/pnas.1018733108

SI Text

Elastic Wave Velocities for Silicon in the Lateral Plane. For the slab orientation in this experiment, the elastic wave propagation will be in the lateral plane defined by the [100] and $[0\bar{1}1]$ vectors (i.e., in the cube-face diagonal). Because silicon is anisotropic, three wave polarizations will exist, one longitudinal and two transverse, with three different speeds all uniquely defined by the stiffness constants of c_{11}, c_{44}, and c_{12} (1)

$$\frac{1}{v_1} = \left(\frac{\rho}{\frac{c_{11}-c_{12}}{2}\cos^2\theta + c_{44}\sin^2\theta}\right)^{1/2}, \quad \text{[S1]}$$

$$\frac{1}{v_2} = \left(\frac{2\rho}{B - \sqrt{B^2 - C}}\right)^{1/2}, \quad \text{[S2]}$$

$$\frac{1}{v_3} = \left(\frac{2\rho}{B + \sqrt{B^2 - C}}\right)^{1/2} \quad \text{[S3]}$$

where

$$B = (c_{11} + c_{12} + 4c_{44})\frac{\cos^2\theta}{2} + (c_{11} + c_{44})\sin^2\theta, \quad \text{[S4]}$$

$$C = (c_{11}c'_{11} - c_{12}^2 - 2c_{12}c_{44})\sin^2 2\theta + 4c_{44}(c'_{11}\cos^4\theta + c_{11}\sin^4\theta),$$

and

[S5]

$$c'_{11} = \frac{c_{11} + c_{12} + 2c_{44}}{2} \quad \text{[S6]}$$

Here, ρ is the mass density of silicon and θ is the angle from the $[0\bar{1}1]$ direction. The v_1 is the pure-shear mode (the wave under consideration), v_2 the quasi-shear, and v_3 the quasi-longitudinal. (Quasi-shear and quasi-longitudinal waves become pure shear and longitudinal for propagation along the high-symmetry axes, such as the [100].)

These equations can be numerically evaluated by using the known values of $\rho = 2.33$ g/cm^3, $c_{11} = 16.57 \times 10^{10}$ N/m^2, $c_{44} = 7.95 \times 10^{10}$ N/m^2, and $c_{12} = 6.39 \times 10^{10}$ N/m^2 for silicon. Fig. S1 shows the results. Here, [011] is used instead of $[0\bar{1}1]$ because they are identical due to the cubic crystal symmetry. The transverse polarizations are 30% slower than longitudinal ones. Moreover, due to crystal anisotropy, the speeds are modified with propagations direction by 10% and 20% for longitudinal and transverse modes, respectively. Note that the known speed of sound for silicon is 8.4 km/s, that is, the velocity of quasi-longitudinal wave along [100].

Projection of an Arbitrary Polarization Vector on the $(\bar{1}14)$ Diffraction Plane. Let us define the orthonormal axes of the reciprocal space as follows:

$$\hat{X} = \frac{[1\bar{3}1]}{\sqrt{11}}, \quad \text{[S7]}$$

$$\hat{Y} = \frac{[13\ 5\ 2]}{\sqrt{198}}, \quad \text{and} \quad \text{[S8]}$$

$$\hat{Z} = \frac{[\bar{1}14]}{\sqrt{18}}. \quad \text{[S9]}$$

Then, the projections of orthonormal slab coordinates, i.e., $\hat{e}_1 = [100]$, $\hat{e}_2 = [011]/\sqrt{2}$, and $\hat{e}_3 = [0\bar{1}1]/\sqrt{2}$ on $\hat{X}, \hat{Y}, \hat{Z}$ are given by

$$\hat{e}_1 = 0.301\hat{X} + 0.924\hat{Y} - 0.236\hat{Z}, \quad \text{[S10]}$$

$$\hat{e}_2 = -0.426\hat{X} + 0.352\hat{Y} + 0.833\hat{Z}, \quad \text{and} \quad \text{[S11]}$$

$$\hat{e}_3 = 0.853\hat{X} - 0.151\hat{Y} + 0.500\hat{Z}. \quad \text{[S12]}$$

An arbitrary polarization vector in the sample coordinate system, $\vec{U} = u_1\hat{e_1} + u_2\hat{e_2} + u_3\hat{e_3}$, can be transformed to the measurement system, as (by Eqs. **S10–S12**)

$$\begin{aligned}\vec{U} = {} & (0.301u_1 - 0.426u_2 + 0.853u_3)\hat{X} \\ & + (0.924u_1 + 0.352u_2 - 0.151u_3)\hat{Y} \\ & + (-0.236u_1 + 0.833u_2 + 0.500u_3)\hat{Z}. \quad \text{[S13]}\end{aligned}$$

For compressional motions (or longitudinal waves), one can measure all three components of $\vec{U}$ by the position of Bragg reflections. Hence, u_1, u_2, u_3 can be uniquely determined by Eq. **S13**. As noted in the text, we do not observe dynamics on the position of high-order-Laue-zone stripes, but only the exponential intensity decay.

For shear motions, the projection rules are the same. From Kikuchi dynamics, one can experimentally measure the $\hat{X}$ and $\hat{Y}$ components; for the shear-horizontal eigenmode of the acoustic waveguide, the vertical polarization is zero (i.e., $u_2 = 0$). In fact, the shear-vertical waves do not totally reflect from the Si–vacuum interface, so they are not expected to propagate inside the slab. Then one can uniquely determine u_1 and u_3 from Eq. **S13**,

$$0.301u_1 + 0.853u_3 = 0.25, \quad \text{[S14]}$$

$$0.924u_1 - 0.151u_3 = 0. \quad \text{[S15]}$$

These equations can be solved for $u_1 = -0.05$ and $u_3 = 0.31$ mrad. The primary polarization is along $u_3 = [0\bar{1}1]$ as we obtained from the phase and amplitude images of the Fourier transform in the main report.

Elastic Waveguide Modes of Shear-Horizontal Waves. The waveguide dispersion relation of a slab is given by Eq. 2 of the manuscript,

$$\omega^2 = v_s^2\left[k_{//}^2 + \left(\frac{n\pi}{b}\right)^2\right] \quad \text{[S16]}$$

where v_s is the transverse wave velocity from Fig. S1, $b = 130$ nm, and n the order of the mode. This equation is plotted in Fig. S2 for $n = 0$, $n = 1$, and $n = 2$. The horizontal dashed line at the experimentally observed frequency of 33 GHz intersects only

the first two dispersion curves, hence it is the $n = 0$ and $n = 1$ modes that can be supported by the slab.

Flexural Motions of the Silicon Slab. One concern might be that the observed dynamic could be a result of the flexural motions of the slab. In order to disregard this possibility, we have calculated the eigenfrequencies of the these modes by means of the finite element analysis. Because the slab had a wedge angle, a numerical computation was the optimum approach.

Fig. S3 depicts the displacements of the first and third flexural eigenmodes of the silicon slab. Frequencies are in the megahertz range, 5 orders of magnitude less than our experimental observations, which dismisses the possibility of measuring these deformations, and consistent with the previously observed time scales of flexural motions in nanostructures (2, 3).

1. Auld B (1973) *Acoustic Fields and Waves in Solids*, (Krieger, Malabar, FL), Vol I.
2. Flannigan DJ, Samartzis PC, Yurtsever A, Zewail AH (2009) Nanomechanical motions of cantilevers: Direct imaging in real space and time with 4D electron microscopy. *Nano Lett* 9:875–881
3. Kwon OH, Park HS, Baskin JS, Zewail AH (2010) Nonchaotic nonlinear motion visualized in complex nanostructures by stereographic 4D electron microscopy. *Nano Lett* 10:3190–3198.

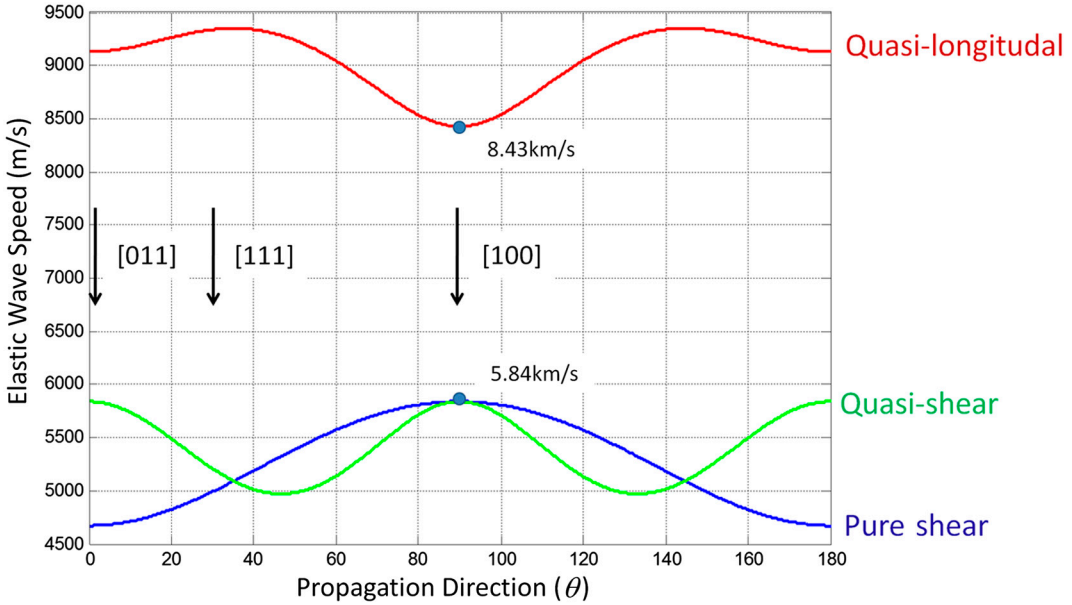

Fig. S1. Elastic wave speeds for three polarizations in crystalline silicon as a function of the propagation direction. The plane of propagation is defined by [011] and [100]. Black arrows indicate the high-symmetry directions.

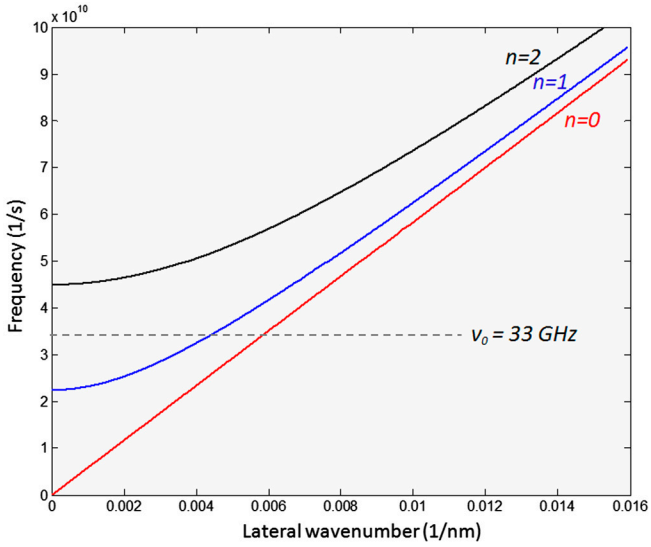

Fig. S2. Dispersion curves of the first three modes of shear-horizontal elastic waves in a silicon slab. The units of the axes are frequency ($\omega/2\pi$) and wavenumber ($k_{//}/2\pi$). The dashed horizontal line indicates the observed resonance frequency.

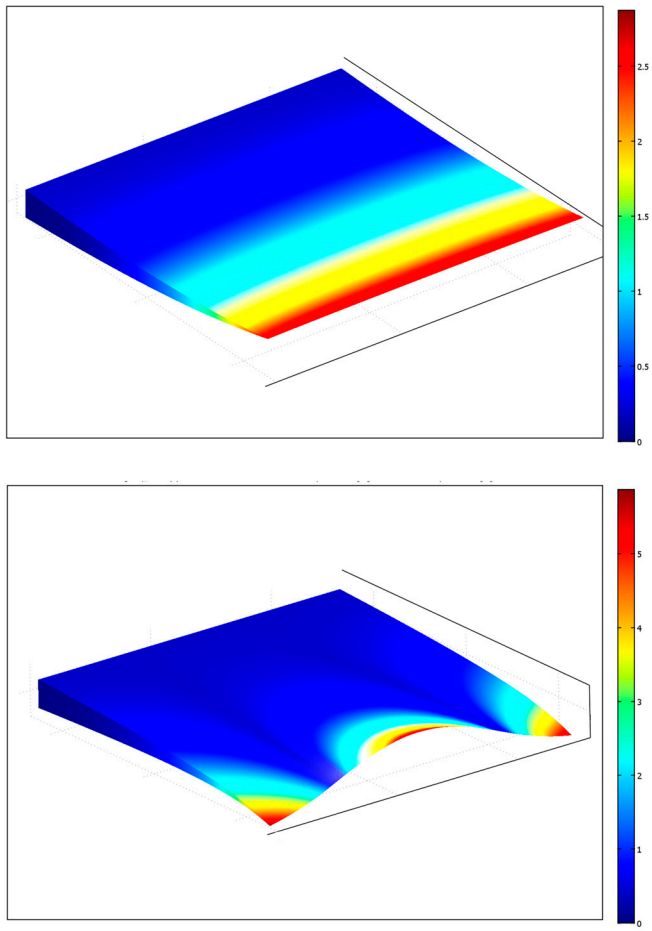

Fig. S3. The first (at 0.3 MHz) and third (at 0.7 MHz) flexural modes of the silicon slab simulated by the finite element method. A commercially available software package (COMSOL) was used. Slab dimensions are 500 × 500 μm and the slab has a 4° wedge. The total displacement is color coded as shown in the color bar.